Rare Metal Materials and Engineering
Volume 52, Issue 2, February 2023
Available online at www.rmme.ac.cn

Science Press

Cite this article as: Chen Lunjiang, Chen Wenbo, Dan Min, et al. Plasma Spheroidization of Ta Powder and Formation Mechanism of Satellite Powder in the Process of Spheroidization[J]. Rare Metal Materials and Engineering, 2023, 52(02): 409-415.

ARTICLE

Plasma Spheroidization of Ta Powder and Formation Mechanism of Satellite Powder in the Process of Spheroidization

Chen Lunjiang[1], Chen Wenbo[2], Dan Min[1], He Yanbin[1], Nie Junwei[1], Zhu Hailong[3], Tong Honghui[1], Jin Fanya[1]

[1] Southwestern Institute of Physics, Chengdu 610041, China; [2] University of South China, Hengyang 421001, China; [3] Shanxi University, Taiyuan 030006, China

Abstract: Micron tantalum powder (Ta) has broad application prospects in biomedical additive manufacturing and other manufacturing fields. The irregular tantalum powder was spheroidized by RF thermal plasma to improve its fluidity. The tantalum powder before and after plasma spheroidization was characterized, and the formation mechanism of satellite powder in the process of spheroidization was analyzed. The results show that the tantalum powder after plasma spheroidization has ideal sphericity and smooth surface, and its Hall fluidity and apparent density are increased from 13.6 $s \cdot (50\ g)^{-1}$ to 6.73 $s \cdot (50\ g)^{-1}$ and from 6.83 $g \cdot cm^{-3}$ to 9.06 $g \cdot cm^{-3}$, respectively. The spheroidization rate and spherical degree of tantalum powder can reach about 95.2% and 0.92, respectively. The formation of satellite powder in the spheroidization process is mainly caused by the collision of droplets, and with the increase in powder feeding rate, the collision probability of droplets increases, resulting in larger particle size of spherical particles due to the droplet condensation.

Key words: thermal plasma; spherical tantalum powders; droplets collision; satellite powders; additive manufacturing

Tantalum (Ta), as one of the most valuable and unique refractory metals, has a series of excellent properties such as good corrosion resistance and strong toughness, malleability (elongation 10%–25%) and great biocompatibility[1–3]. These unique advantages lead to its widespread applications in many fields including medical surgery, dentistry, and aerospace[4]. In the fields of additive manufacturing (AM) of bone trabecular metal implants, in particular, it has been considered as an ideal material to replace the human's bone because of its outstanding biomechanical adaptability. As the key material for AM tantalum implants, micro-sized spherical Ta powder is very hard to prepare and the performance (excellent flowability, lower oxygen content and higher sphericity, etc) is extremely strictly required in the medical implants, which restricts its application in the medical treatment. Traditional preparation methods of spherical powders include rotating electrode[5–6] and atomization method[7–10], which cannot satisfy the requirements for the superior quality of spherical Ta powder due to its extremely high melting point (2996 °C). In recent years, the radio frequency-inductively coupled thermal plasma (RF-ICTP) is one of the most widely applied methods in the preparation of spherical powders and has been extensively used for the spheroidization of irregular refractory metal powders[11–13].

In the past decades, spherical powder has been studied by many researchers using different methods and recently it has increasingly rapid advances in the field of AM. The RF thermal plasma spheroidization method is confirmed as one of the most promising technique for surface shaping of irregular powders because of its higher temperature and longer heating residence time, which can ensure more effective melting of refractory metal powders[12–13]. It is now well established from

Received date: April 01, 2022
Foundation item: National Natural Science Foundation of China (11875039, 52173041); Innovation Program of SWIP (202102XWCXYD001); Sichuan Science and Technology Program (2019YFG0444)
Corresponding author: Jin Fanya, Ph. D., Researcher, Southwestern Institute of Physics, Chengdu 610041, P. R. China, Tel: 0086-28-82820865, E-mail: yafanjin@swip.ac.cn

a variety of studies that the process of particle melting and droplet solidification is very critical to the performance of spherical powders in thermal plasma spheroidization. Recently, some researchers are focused on the preparation of spherical refractory powders (W, Mo, ZrO_2, etc) using the RF-ICTP technologies. Hao et al[14] reported that the spheroidization process is a combination of melting, sintering and solidification, and proved that the best spheroidization can be achieved when the plasma power is 43 kW for molybdenum (Mo) powder spheroidization. He et al[15] presented that sphericity of coarse particles is evidently higher than that of fine particles, and that the sphericity could be optimized by adjusting the gas flow in tungsten powder spheroidization. Du et al[16] found that some spherical particles have lines on their surfaces due to insufficient heating in the RF thermal plasma spheroidization. Up to now, far too little attention has been paid to the preparation and characterization of various spherical powders and the influence of plasma operation parameters on sphericity and spheroidization rate from the previous published studies[17–21]. Satellite powder is one of the most frequently stated problems according to the results of present researches[20–22]. Surprisingly, the problem has received scant attention and the formation process of satellite powder in thermal plasma spheroidization has seldom been reported.

In this study, irregular Ta powder was spheroidized by RF inductively coupled thermal plasma (RF-ICTP) process and the characteristics of the powder after plasma treatment were investigated. The formation mechanism and influencing factors of satellite powders were explored in the RF-ICTP process. Finally, the relationship between satellite powder ratio and powder feeding rate was discussed. This study can provide a new insight into the preparation of high-performance spherical Ta powder for additive manufacturing.

1 Experiment

1.1 Materials and experiment set-up

The experimental tantalum powder (10 – 90 μm, purity> 99.9%) from Zhuzhou Cemented Carbide Group Co., Ltd as the raw material was prepared by sodium (Na) reduction method. Laboratory apparatus used in this work was a RF-ICTP powder spheroidization set-up, consisting of a 3±0.5 MHz high-frequency electron tube oscillator with 100 kW power, a RF plasma torch with water-cooled ceramic tube and copper coil, a system of gas and powder feeder, powder spheroidization and filter chamber, spherical powder container, and the vacuum system. The schematic illustration of the experimental set-up is shown in Fig.1.

1.2 RF-ICTP spheroidization of tantalum powder

The typical experimental processes of Ta powder spheroidization can be briefly described here. Before the experiment, a vacuum degree of 1×10^{-1} Pa was created by the vacuum pump and then the system pressure was filled into 1.013×10^5 Pa (atmospheric pressure) with pure argon (purity> 99.99%) to reduce the oxygen content in the spheroidization process. After the chamber pressure was evacuated to

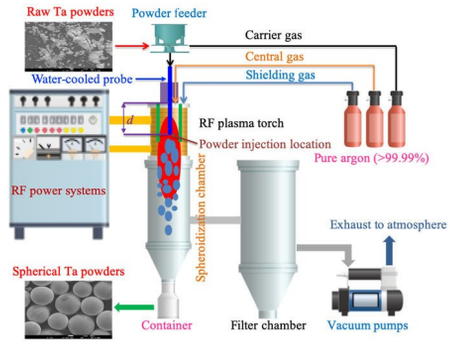

Fig.1 Schematic illustration of experimental set-up and spheroidization

approximately 0.035 MPa, argon as a plasma-forming medium was inputted into the RF plasma torch with central gas of 25 L/min (slpm) and shielding gas of 20 L/min (slpm). When the RF oscillator was turned on and the power was increased slowly, a strong arc discharge formed in the ceramic tube because of the electromagnetic energy from the RF coil. After that, the gas flow of central gas and shielding gas was then increased immediately to preserve a stable thermal plasma jet. Then, the experimental Ta powders with the carrier gas (argon) were fed into the plasma reaction region axially through a powder feeder and a water-cooled probe inserted into the plasma jets. Under the action of high temperature, the solid tantalum particles were heated and melted rapidly into liquid droplets with extremely high sphericity due to the surface tension. Those droplets, once escaped from the plasma jet zone, were solidified to form the spherical particles immediately in the quenching chamber. Finally, the spherical Ta powders were accumulated in the collection container at the bottom of spheroidization chamber. The typical experimental parameters for tantalum powders spheroidization with RF-ICTP are listed in Table 1.

Surface morphologies and microstructural characteristics of the samples were observed by a field emission scanning electron microscope (FESEM, JSM-7500F, JEOL, Japan). The particle size distribution of Ta powders was investigated on a laser particle size instrument (HELOS-RODOS/M, Germany). The phase structure was measured by X-ray diffractometer (XRD, EMPYREAN, Branch, Netherland) with Cu Kα

Table 1 Experimental parameters for Ta powders spheroidization with RF-ICTP

Parameter	Value
RF voltage/kV	7
RF current/A	7.8
Reaction chamber pressure/kPa	40
Central gas of Ar/L·min^{-1} (slpm)	35
Shielding gas of Ar/L·min^{-1} (slpm)	85
Carrier gas of Ar/L·min^{-1} (slpm)	1
Powder feeding rate/g·min^{-1}	25–70
Powder injection location, *d*/mm	60

radiation between 10° and 90°. The Hall flowmeter and Scott-method were used to determine the flowability (GB/T 1482–2010) and apparent density (ASTM B 329, GB/T 1479.1–2011) of tantalum powders, respectively. The spheroidization ratio χ or satellite ratio γ of tantalum powder after plasma treatment was estimated approximately from FESEM images based on the statistical principle of random sampling and spherical degree σ associated with particle size can be obtained by the following equations:

$$\chi \text{ or } \gamma = C_b/C_a \times 100\% \quad (1)$$

$$\sigma = 4\pi\left(\frac{3V_p}{4\pi}\right)^{\frac{2}{3}} \Big/ S_p \quad (2)$$

where C_a and C_b are the average value of the total number of spherical particles and satellite particles, respectively, counted from the FESEM images of the prepared Ta powders by multiple random sampling; V_p and S_p is the particle volume and surface area calculated by the particle size of D_{50} from the test of laser particle size for spherical Ta powders, respectively.

2 Results and Discussion

2.1 Effect of plasma spheroidization on surface methodology and microstructure

The raw Ta powders used in this experiment present an irregular surface morphology and some agglomerations of ultrafine particles, as shown in Fig. 2a and Fig. 2b, in accordance with the characteristics of Na reducing powder. The range of size distribution with the median particle size D_{50}=36.99 μm is wide, and the apparent density and Hall flowability are 6.83 g·cm^{-3} and 13.6 s·(50 g)$^{-1}$, respectively, as shown in Fig.2c.

At a powder feeding rate of 25 g·min^{-1}, the raw Ta powder is spheroidized under the listed experimental parameters in Table 1. The FESEM observations in Fig. 3 illustrate that the majority of prepared powders with excellent dispersion of single particles after plasma treatment is spherical and the spheroidization ratio is $\chi \approx 95\%$ due to the action of high temperature. The prepared powders with a good spherical degree of $\sigma \approx 0.92$ estimated from Eq. (2) present a smooth surface, as shown in Fig. 3a–3e. It is also demonstrated that a small fraction of prepared powders are still not melted (marked by A), or partially melted (marked by B) in spite of the extremely high temperature of thermal plasma, as shown in Fig. 3b. The uneven surface tension of droplets in all directions may form pits on the surface of spherical powder. All of these results are related to the behavior of particles in plasma. In fact, the heating and melting of particles in plasma spheroidization are mainly related to plasma temperature and residence time of particles in the plasma. Once those particles are far away from the high temperature zone or have a short residence time before flying out of plasma jet, they will not obtain sufficient energy to be heated and melted effectively in the process of plasma spheroidization.

The single and most striking observation to emerge from Fig. 3e is those satellite particles on the surface of spherical powders, which result in a coarse surface, as presented in Fig. 4a. In plasma spheroidization, those tiny particles in the raw powder may be evaporated to form the nano-particles due to the excessive heating absorption from plasma in a short time, which can be adhered on the surface of spherical solid particles or droplets after solidification because of the nano-effect in region A of Fig. 4b. Furthermore, the collisions of droplets in motion process occurring at the solidification zone

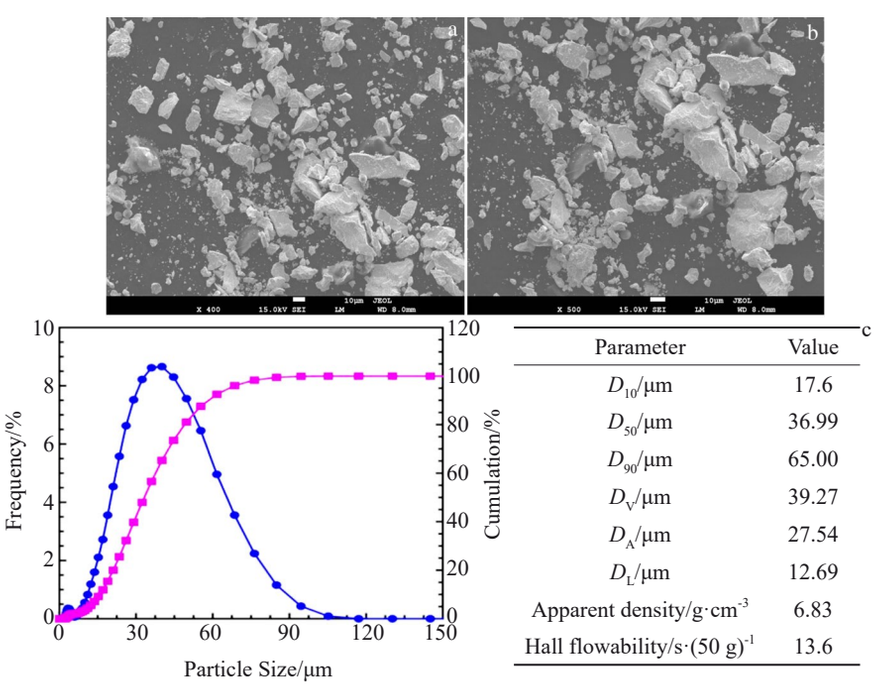

c

Parameter	Value
D_{10}/μm	17.6
D_{50}/μm	36.99
D_{90}/μm	65.00
D_V/μm	39.27
D_A/μm	27.54
D_L/μm	12.69
Apparent density/g·cm^{-3}	6.83
Hall flowability/s·(50 g)$^{-1}$	13.6

Fig.2 FESEM morphologies (a, b) and particle size distribution (c) of raw tantalum powder

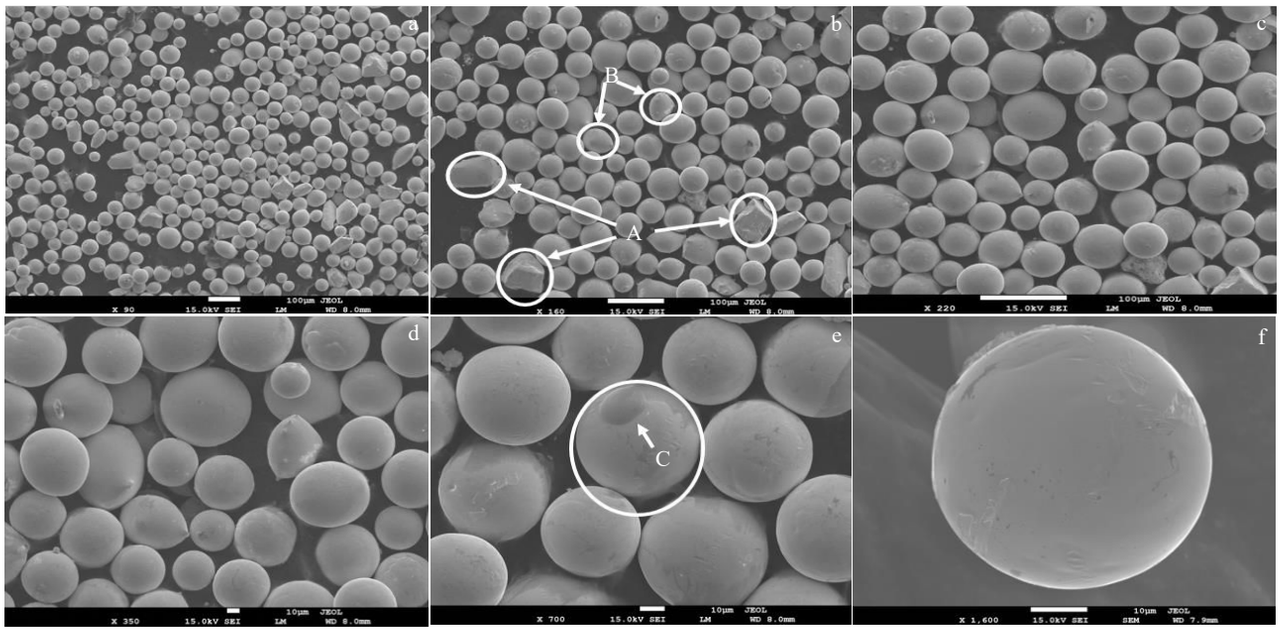

Fig.3 FESEM morphologies of spherical Ta powders after plasma treatment

may form the satellite powders in region B of Fig. 4b (or region C of Fig.3e).

The phase structure and oxidization of Ta powders before and after RF-ICTP processing were characterized by X-ray diffraction, as shown in Fig.5. It can be clearly seen from the data in Fig. 5 that the main characteristics associated with oxidization are detected at the diffraction peaks of (001), (1110), (141) and (1111), indicating that the Ta powders are still oxidized easily at high temperature in our setup even if

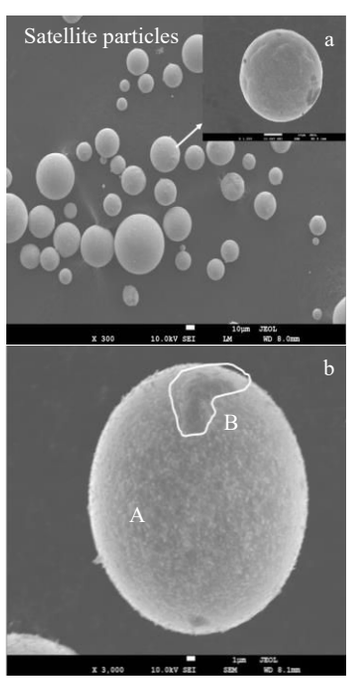

Fig.4 FESEM morphologies of satellite Ta powders in the final spherical products

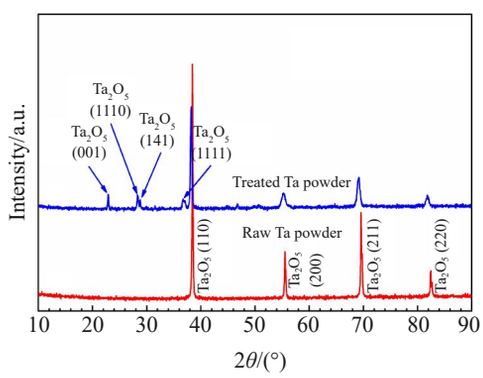

Fig.5 XRD patterns of raw Ta powders and plasma treated Ta powders

the system has been cleaned and replaced with pure argon before the experiment. The phase structure of raw tantalum powder has a body centered structure indicated from the diffraction peaks of (110), (200), (211) and (220), while that of spheroidized tantalum powder appears with the orthorhombic structure phase of Ta_2O_5. The oxidation phenomenon in the RF-ICTP spheroidization can be improved by increasing the vacuum degree of the system.

2.2 Formation process of satellite powder in plasma spheroidization

In the heating and movement process of Ta powder, portions of the small particles are evaporated to steam due to the low heat required and then recrystallized to adhere on the surface of spherical particles, while the droplets melted from the large particles collide with each other to form the satellite powders, as shown in Fig. 6. As mentioned above, the formation of satellite powders is mainly from the evaporation and recrystallization of small-sized particles and the collision

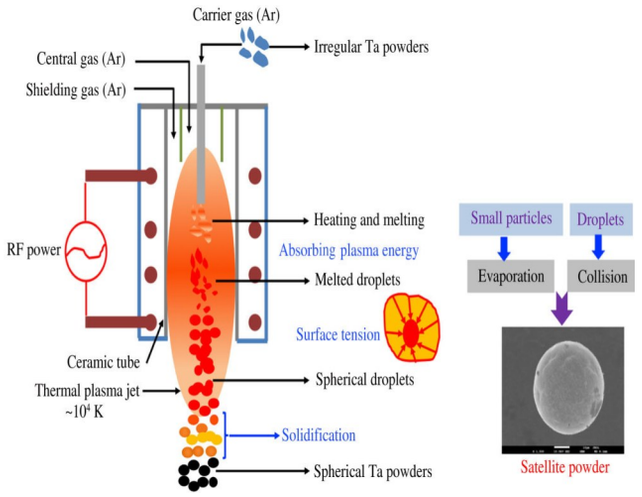

Fig.6 Process of RF plasma spheroidization and formation of satellite powder

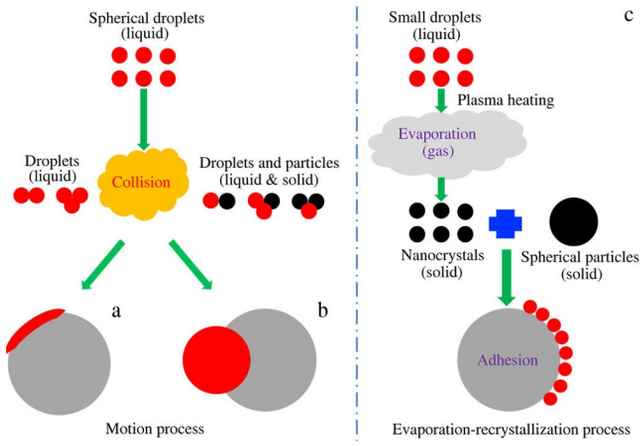

Fig.7 Formation mechanism and classifications of satellite powders in RF-ICTP spheroidization: (a) cladding, (b) surface contact, and (c) point contact

of droplets, which can be divided into three classifications from FESEM morphologies of the final spherical products: cladding, surface contact and point contact, as presented in Fig. 7. The droplets with high temperature have not yet been solidified and struck into the solidified powder rapidly to form the cladding type (Fig. 7a); the pre-solid droplets with high temperature hit on the surface of liquid or solidified powder promptly to form the type of surface contact (Fig. 7b), while the point contact type often occurs in the evaporation and condensation process of droplets on the surface of solid particles (Fig.7c).

2.3 Effect of powder feeding rate on properties of prepared products

FESEM morphologies at different powder feeding rates M are presented in Fig. 8. It can be seen that the plasma treated Ta powders have perfect sphericity and smooth surface at a low feeding rate, and the spheroidization ratio can reach up to about 92.5% at M=36 g·min^{-1}. When the powder feeding rate increases, more collision among the droplets in the plasma jets results in a low spheroidization and a high satellite ratio of the final prepared powders. As a result, the diameter of final powder is increased, which results in a wide distribution of particle size due to droplet collision and condensation at a high feeding rate, as listed in Table 2.

The perfect flow ability and apparent density of powders are significantly important indexes for AM. The variation of those properties with spheroidization ratio of Ta powders is shown in Fig. 9. It is illustrated that the higher the spheroidization ratio, the more satisfying the properties of spherical powders, and the Hall flowability and apparent density can reach up to about 6.73 s·(50 g)$^{-1}$ and 9.06 g·cm^{-3},

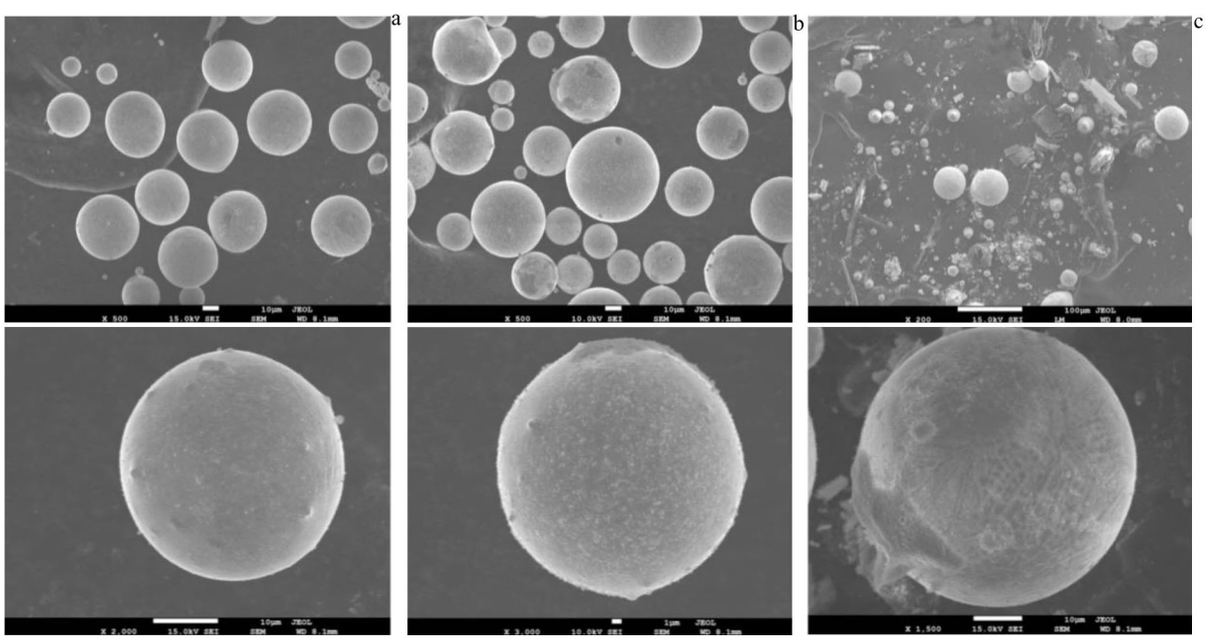

Fig.8 FESEM morphologies of spherical products at different powder feeding rates: (a) M=36 g·min^{-1}, (b) M=52 g·min^{-1}, and (c) M=65 g·min^{-1}

Table 2 Particle size distribution of plasma treated Ta powders

Feeding rate/g·min^{-1}	D_{10}/μm	D_{50}/μm	D_{90}/μm
36	17.2	37.6	76.9
52	13.4	57.3	120
65	23	71.2	219

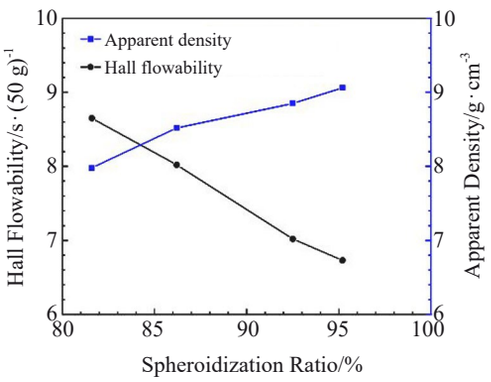

Fig.9 Effect of spheroidization ratio on properties of plasma prepared Ta powder

respectively. Although the satellite powder forms in thermal plasma spheroidization, the properties of spherical Ta powders are significantly improved compared with those of raw Ta powders and the improvements are beneficial for additive manufacturing.

As mentioned above, the formation of satellite powder often occurs in the process of droplet solidification. The longer the condensation time or the slower the velocity of the droplets, the higher the collision probability among the droplets, which will lead to more satellite powders. In addition, the formation mechanism of satellite powders is also related to the concentration of the droplets (powder feeding rate) in the space of plasma discharge. The satellite powder will result in a poor flowability and a low apparent density due to its rough surface. Hence, on the premise of complete melting of the particles, a lower powder feeding rate as much as possible in plasma spheroidization will be beneficial to reduce the satellite ratio, and the condensation time can be adjusted by the plasma operation parameters (including plasma power, gas flow and pressure, etc).

3 Conclusions

1) The formation of satellite powder will affect the properties of plasma-spheroidized Ta powder, and the collision of droplets and the adhesion of nanoparticles are the main reasons for the formation of satellite powders.

2) The increase in powder feeding rate results in a larger particle size of spherical Ta powder, which can lead to an increased satellite rate due to the increasing collision probability in the process of plasma spheroidization, and some powders are oxidized to Ta_2O_5 in the spheroidization of tantalum powder. Therefore, it is recommended to control the powder feeding rate at or below 25 g·min^{-1} for the raw tantalum powders with 10–90 μm in size.

References

1 Dong Chao, Bi Xianlei, Yu Jingui *et al*. *Journal of Alloys and Compounds*[J], 2019, 781: 84
2 Kim Youngmoo, Lee Dongju, Hwang Jaewon *et al*. *Materials Characterization*[J], 2016, 114: 225
3 Thakre Piyush, Yang Vigor. *Journal of Propulsion and Power*[J], 2012, 25: 40
4 Sungai Craig, Abid Aamir. *Metal Powder Report*[J], 2018, 73(6): 316
5 He Weiwei, Liu Yong, Tang Huiping *et al*. *Materials & Design*[J], 2017, 132: 275
6 Yin J O, Chen G, Zhao S Y *et al*. *Journal of Alloys and Compounds*[J], 2017, 713: 222
7 Anderson Iver E, Terpstra Robert L. *Materials Science and Engineering A*[J], 2002, 326(1): 101
8 Chen Gang, Tan Ping, Zhao Shaoyang *et al*. *Key Engineering Materials*[J], 2016, 704: 287
9 Ünal Rahmi. *Journal of Materials Processing Technology*[J], 2006, 180(1–3): 291
10 Dhokey N B, Walunj M G, Chaudhari U C. *Advanced Powder Technology*[J], 2014, 25: 795
11 Wang J J, Hao J J, Guo Z M *et al*. *Rare Metals*[J], 2015, 34: 431
12 Jiang X L, Boulos M I. *Transactions of Nonferrous Metals Society of China*[J], 2006, 16(1): 13
13 Cao Yongge, Zhao Chong, Ma Chaoyang *et al*. *Rare Metal Materials and Engineering*[J], 2019, 48(2): 446
14 Hao Zhenhua, Fu Zhenhua, Liu Jintao *et al*. *International Journal of Refractory Metals and Hard Materials*[J], 2019, 82: 15
15 He J, Bai L, Jin H *et al*. *Powder Technology*[J], 2016, 302: 288
16 Du Wenhao, Shi Qi, Wu Anru *et al*. *Rare Metal Materials and Engineering*[J], 2021, 50(12): 4457
17 Wei W H, Wang L Z, Chen T *et al*. *Advanced Powder Technology* [J], 2017, 28: 2431
18 Károly Z, Mohai I, Klébert S *et al*. *Powder Technology*[J], 2011, 214: 300
19 Kobayashi N, Kawakami Y, Kamada K *et al*. *Thin Solid Films* [J], 2008, 516: 4402
20 Li Y L, Ishigaki T. *Journal of the America Ceramic Society*[J], 2001, 84: 1929
21 Li R, Qin M, Huang H *et al*. *Advanced Powder Technology*[J], 2017, 28: 2158
22 Xiong H B, Zheng L L, Li L *et al*. *International Journal of Heat & Mass Transfer*[J], 2005, 48: 5121

钽粉等离子体球化及其球化过程中卫星粉的形成机制

陈伦江[1]，陈文波[2]，但　敏[1]，贺岩斌[1]，聂军伟[1]，朱海龙[3]，童洪辉[1]，金凡亚[1]

(1. 核工业西南物理研究院，四川 成都 610041)

(2. 南华大学，湖南 衡阳 421001)

(3. 山西大学，山西 太原 030006)

摘　要：微米级钽粉（Ta）在生物医疗增材制造和其它制造领域具有广阔的应用前景。采用射频热等离子体对不规则钽粉进行球化处理以改善其流动性，对等离子体球化处理前后的钽粉进行了表征，并分析了球化过程中卫星粉的形成过程与机制。结果表明，经等离子体球化后的钽粉具有较为理想的球形度和光滑的表面，其霍尔流动性和表观密度分别从13.6 s·(50 g)$^{-1}$提高到6.73 s·(50 g)$^{-1}$和6.83 g·cm^{-3}提升至9.06 g·cm^{-3}，钽粉的球化率和球形度分别可约达95.2%和0.92；球化过程中卫星粉的形成主要是因液滴的碰撞所致，且随着送粉速度的增加，液滴碰撞概率增大，液滴的凝并使球形颗粒的粒径增大。

关键词：热等离子体；球形钽粉；液滴碰撞；卫星粉；增材制造

作者简介：陈伦江，男，1985年生，博士（后），副研究员，核工业西南物理研究院，四川 成都 610041，电话：028-82820865，E-mail：lunjiangchen@163.com